

# miR-125a-5p/miR-125b-5p contributes to pathological activation of angiotensin II-AT1R in mouse distal convoluted tubule cells by the suppression of Atrap

Received for publication, October 16, 2023, and in revised form, November 6, 2023. Published, Papers in Press, November 21, 2023.

<https://doi.org/10.1016/j.jbc.2023.105478>

Keigo Hirota<sup>1</sup>, Akio Yamashita<sup>2,\*</sup> , Eriko Abe<sup>1</sup>, Takahiro Yamaji<sup>1</sup>, Kengo Azushima<sup>1</sup>, Shohei Tanaka<sup>1</sup>, Shinya Taguchi<sup>1</sup>, Shunichiro Tsukamoto<sup>1</sup>, Hiromichi Wakui<sup>1</sup>, and Kouichi Tamura<sup>1,\*</sup> 

From the <sup>1</sup>Department of Medical Science and Cardiorenal Medicine, Yokohama City University Graduate School of Medicine, Yokohama, Japan; <sup>2</sup>Department of Investigative Medicine, Graduate School of Medicine, University of the Ryukyus, Okinawa, Japan

Reviewed by members of the JBC Editorial Board. Edited by Kirill Martemyanov

The renin-angiotensin system plays a crucial role in the regulation of blood pressure. Activation of the angiotensin II (Ang II)-Ang II type 1 receptor (AT1R) signaling pathway contributes to the pathogenesis of hypertension and subsequent organ damage. AT1R-associated protein (ATRAP) has been identified as an endogenous inhibitory protein of the AT1R pathological activation. We have shown that mouse Atrap (Atrap) represses various Ang II-AT1R-mediated pathologies, including hypertension in mice. The expression of human ATRAP (ATRAP)/Atrap can be altered in various pathological states in humans and mice, such as Ang II stimulation and serum starvation. However, the regulatory mechanisms of ATRAP/Atrap are not yet fully elucidated. miRNAs are 21 to 23 nucleotides of small RNAs that post-transcriptionally repress gene expression. Single miRNA can act on hundreds of target mRNAs, and numerous miRNAs have been identified as the Ang II-AT1R signaling-associated disease phenotype modulator, but nothing is known about the regulation of ATRAP/Atrap. In the present study, we identified miR-125a-5p/miR-125b-5p as the evolutionarily conserved miRNAs that potentially act on ATRAP/Atrap mRNA. Further analysis revealed that miR-125a-5p/miR-125b-5p can directly repress both ATRAP and Atrap. In addition, the inhibition of miR-125a-5p/miR-125b-5p resulted in the suppression of the Ang II-AT1R signaling in mouse distal convoluted tubule cells. Taken together, miR-125a-5p/miR-125b-5p activates Ang II-AT1R signaling by the suppression of ATRAP/Atrap. Our results provide new insights into the potential approaches for achieving the organ-protective effects by the repression of the miR-125 family associated with the enhancement of ATRAP/Atrap expression.

Hypertension is one of the most common complications worldwide, predisposing health problems and affecting various organs. In 2010, 31.1% of the world's adult population (1.39 billion people) had hypertension (1). Among the pathways

involved in the development of hypertension, the renin-angiotensin system (RAS) plays a crucial role; particularly, the angiotensin II (Ang II)-Ang II type 1 receptor (AT1R) signaling pathway directly affects the arterial constriction (2), tubular sodium reabsorption (3–5), the release of aldosterone, a mineralocorticoid (6, 7), and the induction of insulin resistance (8). Activation of the Ang II-AT1R signaling pathway at local sites contributes to the pathogenesis of hypertension, renal diseases associated with oxidative stress, and fibrotic conditions (9, 10). Consequently, RAS inhibitors are widely utilized as key drugs due to their antihypertensive and organ-protective effects (11). However, excessive inhibition of the RAS has been associated with adverse events including hypotension, hyperkalemia, and renal damage (12, 13).

AT1R-associated protein (ATRAP/Atrap) is identified as a direct binding protein of AT1R. ATRAP/Atrap acts as an endogenous inhibitory protein of the pathological AT1R hyperactivation at local tissue sites (14–18). For instance, Atrap overproduction (transgenic mice) or depletion (knockout mice) displays repressive or enhancement effects for Ang II-AT1R-mediated hypertension, cardiac hypertrophy, vascular injury, and insulin resistance by blocking pathological activation of AT1R without the alteration of baseline status. Hence, ATRAP/Atrap is a potential therapeutic target of pathological AT1R signaling activation without excessive inhibition.

Understanding how the ATRAP/Atrap expression is regulated is essential because of its protective function against harmful Ang II-AT1R signaling. The research shows that the ATRAP/Atrap expression can be altered in various pathological states in mouse (19–23) and human (10, 24, 25). For example, the Atrap protein degrades in response to the Ang II stimulation in various cells and organs, probably through the proteasome pathway (21, 26, 27). However, ATRAP protein does not have a lysine residue in the putative ubiquitination site. In addition, miR-376a and miR-135a act on and repress rat Atrap mRNA in neurons (28). However, these two miRNAs are expressed specifically in neurons and are not found in kidney tissue.

miRNAs are 21~23 nucleotide noncoding RNAs that post-transcriptionally repress hundreds of target mRNAs. Drosha

\* For correspondence: Akio Yamashita, [akyama21@med.u-ryukyu.ac.jp](mailto:akyama21@med.u-ryukyu.ac.jp); Kouichi Tamura, [tamukou@yokohama-cu.ac.jp](mailto:tamukou@yokohama-cu.ac.jp).

## miR-125 inhibition represses angiotensin II signaling

and Dicer are the miRNA-processing enzymes that are required for the maturation of miRNAs. After Drosha- and Dicer-mediated processing, miRNAs are loaded into the Argonaute (AGO) family of proteins, the active part of the RNA-induced silencing complex, binding the target mRNA strand complementary in the cytoplasm, inducing mRNA exoribonucleolytic degradation and translational repression (29–31). As enhancement of ATRAP/Atrap can repress pathogenic activation of the Ang II–AT1R signaling, the identification of evolutionarily conserved miRNAs acting on ATRAP/Atrap would be intriguing to define new therapeutic target of the Ang II–AT1R signaling. Consistent with this view, numerous miRNAs have been identified as the Ang II–AT1R signaling–associated disease phenotype modulators (32–34). Among these miRNAs, the miR-125 family plays critical roles in the growth, development, and incidence of cardiovascular diseases as well as various cancers (35–37).

In this study, we hypothesized that miRNA plays a role in regulating Atrap expression following Ang II treatment in renal tubular cells, and that this regulation is evolutionarily conserved. Our analysis revealed that miR-125a-5p and miR-125b-5p can directly repress both Atrap and ATRAP. Furthermore, inhibition of miR-125a-5p–miR-125b-5p resulted in the suppression of Ang II–AT1R signaling activation in mouse distal convoluted tubule (mDCT) cells. Our results should provide new insights into potential approaches for achieving organ-protective effects by repressing the miR-125 family associated with enhancing ATRAP/Atrap expression.

### Results

#### *Cloning, characterization, and the Ang II stimulation of mDCT cells*

ATRAP/Atrap is highly expressed in renal tissues, especially in the proximal and distal tubules (10). In addition, the inhibitory role of Atrap for the pathological Ang II–AT1R signaling is investigated in a mouse model (15). Therefore, we plan to analyze the regulatory mechanisms of Atrap in mDCT cells. Due to the heterogeneity and instability of the cell phenotype, we have cloned and characterized mDCT cells (10, 38). We selected mDCT\_clone 2E because it showed higher expression of distal convoluted tubular cell markers (Figs. 1A and S1, A–D). From now on, we will refer to it as “mDCT.” We then observed the response of the Ang II treatment for 6 h. Consistent with previous reports (10), the mDCT cells showed sensitivity to Ang II, which resulted in increased expression of  $\alpha$ ENaC (alpha epithelial sodium channel) and transforming growth factor beta (TGF $\beta$ ) mRNAs, both downstream targets of AT1R signaling. In addition, they increased the expression of Atrap mRNA (as seen in Fig. 1, B and C) but decreased the expression of Atrap protein in these cells (as observed in Figs. 1D, S1E, and S5).

#### *miRNAs repress the expression of Atrap in mDCT cells*

In mDCT cells, Ang II–AT1R caused an increase in Atrap mRNA and a decrease in Atrap protein. This indicated the presence of post-transcriptional regulation of Atrap

expression. To investigate this mechanism, we analyzed the general effect of miRNAs on endogenous Atrap expression by repressing miRNAs with siRNA-mediated Drosha and Dicer knockdown (31). Knockdown of Drosha or Dicer was validated by RT–quantitative PCR (qPCR; Fig. 2A). And an increase in endogenous Atrap protein expression was observed (Figs. 2B, S2A, and S5). Next, we developed an mDCT cell line expressing the exogenous Hibit (a split Nanoluc fragment)-tagged Atrap gene under the doxycycline (Dox)-dependent exogenous promoter (mDCT\_Hibit-Atrap gene) (39) (Fig. 2, C and D). Using this cell line, we investigated the post-transcriptional effects of Drosha knockdown nor Dicer knockdown. Our results showed that the knockdown of either Drosha or Dicer resulted in an increase in Hibit-Atrap expression transcribed from an exogenous promoter, for a duration of 8 h (Fig. 2E). These results indicated that miRNAs have the potential to repress Atrap protein expression in mDCT cells.

#### *Identification of miR-125a-5p/miR-125b-5p as an evolutionarily conserved direct repressor of Atrap expression*

To identify specific miRNAs that act on both Atrap and ATRAP mRNAs and are abundantly expressed in the kidney, we examined the predicted miRNAs using two databases, ENCORI (40) and miTED (41) (Fig. 3A, see *Experimental procedures* section in detail). As a result, we identified four candidate miRNAs: miR-34a-5p, miR-125a-5p, miR-125b-5p, and miR-874-3p, which may act on Atrap–ATRAPP mRNA in renal tubules (Fig. 3A). The previously reported miRNAs targeting rat Atrap mRNA were excluded as candidates because miR-135a and miR-376a are less expressed in the kidney, and miR-370, which targets mouse Atrap mRNA, has no target site in ATRAPP mRNA (28, 42).

To determine the effect of the four candidate miRNAs on Atrap mRNA, we employed synthetic tough decoy (S-TuD), an miRNA inhibitor (Fig. S2B) (43). As shown in Figure 4A, only the miR-125a-5p inhibitor was able to enhance the Hibit-Atrap protein expression in mDCT\_Hibit-Atrap gene cells (Fig. 4A). Note that the miR-125a-5p inhibitor could not discriminate between miR-125a-5p and miR-125b-5p, thus inhibiting both miRNAs. In addition, the miR-125a-5p inhibitor was found to increase the expression of exogenous Hibit-Atrap mRNA (Fig. 4B). These results indicated that miR-125a-5p–miR-125b-5p can repress both Atrap mRNA and protein expression at the post-transcriptional mRNA level. Furthermore, the inhibitors of miR-34a-5p and miR-874-3p did not increase Atrap expression. However, a single gene is regulated by multiple miRNAs (29, 30), thus miR-34a-5p and miR-874-3p might act in different cells/tissues and conditions.

Next, we analyzed whether miR-125a-5p/miR-125b-5p can directly repress Atrap expression or not. For this purpose, we introduced a point mutation of the miR-125a-5p/miR-125b-5p targeting sequence, which was replaced by a complementary sequence, into the Hibit-Atrap reporter gene and stably expressed it in mDCT cells (mDCT\_mut-Hibit-Atrap gene) (Fig. 4C). We then evaluated the effects of the miR-125a-5p

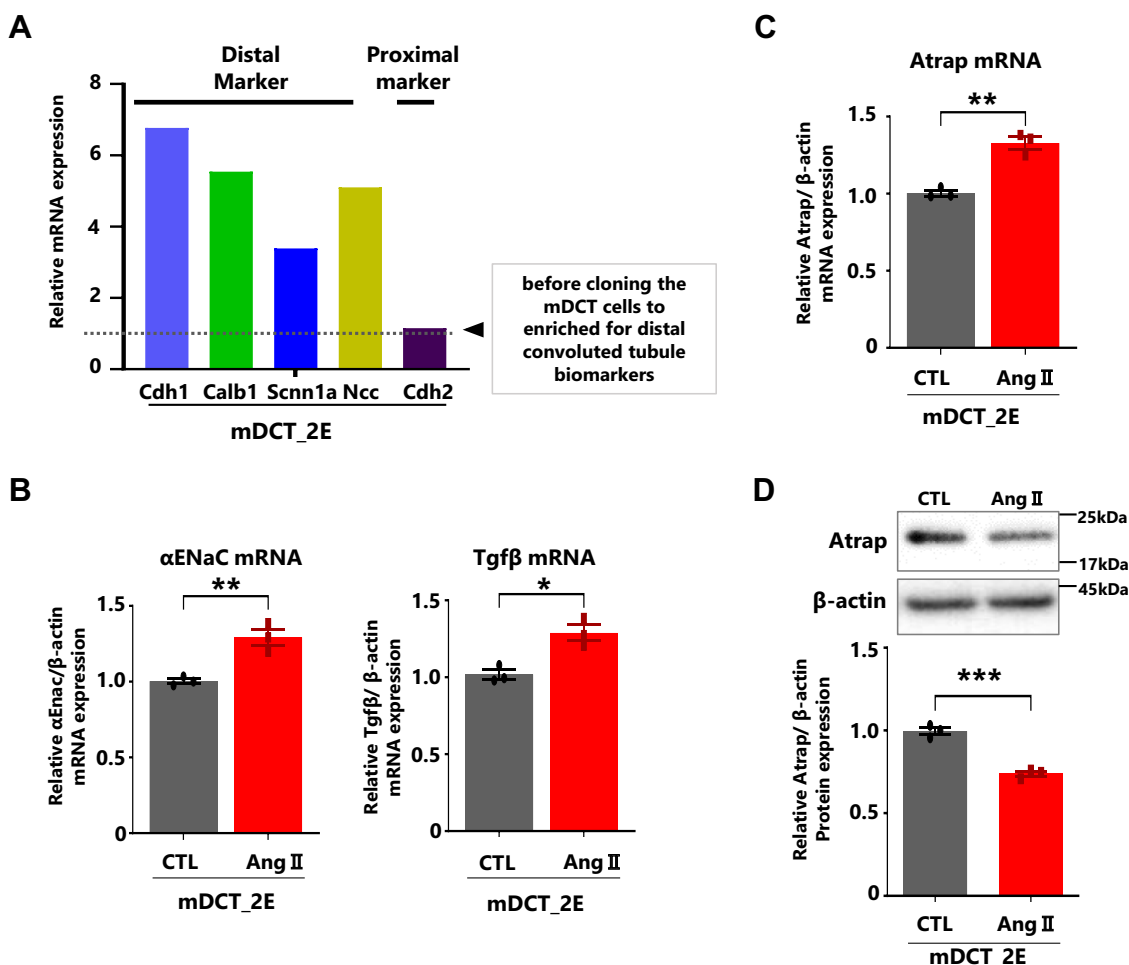


**Figure 1. Cloning, characterization, and the Ang II stimulation to the mouse distal convoluted tubular (mDCT) cells.** Comparison of mRNA expression levels of distal and proximal tubular markers in the mDCT\_2E cells, and the response to Ang II treatment after 6 h. *A*, the relative mRNA levels of distal and proximal tubular markers in mDCT\_2E cells as determined by RT-qPCR, normalized to β-actin. The mRNA levels in mDCT cells before cloning were set to 1 ( $n = 1$ ). *B*, reactivity of Tgfβ and αENaC, the downstream gene of the AT1R signaling. The relative mRNA levels of αENaC and TGFβ were determined by RT-qPCR, normalized to β-actin ( $n = 3$ ). The mRNA levels obtained without Ang II (control; CTL) were set to 1. *C*, reactivity of Atrap mRNA. The relative mRNA levels of Atrap were determined by RT-qPCR, normalized to β-actin ( $n = 3$ ). The mRNA levels obtained without Ang II (CTL) were set to 1. *D*, reactivity of protein. The relative protein levels by Western blotting analysis, normalized to β-actin ( $n = 3$ ). The protein levels obtained without Ang II (CTL) were set to 1. Data were obtained with three biologically independent experiments except (*A*). Values represent the means ± standard error. \* $p < 0.05$ , \*\*\* $p < 0.001$  versus CTL (Ang II 0 μM) group. Data were analyzed *via* the unpaired *t* test. All preprocessing original Western blot data are shown in Fig. S5. αENaC, alpha epithelial sodium channel; Ang II, angiotensin II; AT1R, Ang II type 1 receptor; Atrap, mouse Atrap; qPCR, quantitative PCR; TGFβ, transforming growth factor beta.

inhibitor on mut-Hibit-Atrap expression. Our results indicated that the mutation of miR-125a-5p-miR-125b-5p targeting sequence became insensitive to the miR-125a-5p inhibitor (Fig. 4D). This suggested that miR-125a-5p/miR-125b-5p directly acted on Atrap mRNA and repressed its expression.

To validate the evolutionarily conserved effect of the miR-125a-5p inhibitor on the expression of endogenous Atrap and ATRAP, we transfected the miR-125a-5p inhibitor into mDCT cells or human cloned immortalized renal proximal tubule epithelial cells (ciRPTECs) (24). The results showed that the miR-125a-5p inhibitor enhanced endogenous Atrap/ATRAP protein expression in both mDCT cells and ciRPTECs (Figs. 4, E and F, S2, D and E, and S5). Taken together, these results indicated that miR-125a-5p/miR125b-5p-mediated Atrap/ATRAP repression is evolutionarily conserved between mouse and human.

#### Ang II promoted Atrap mRNA accumulation by repressing miR-125a-5p/miR125b-5p expression

After observing an increase in Atrap mRNA and a decrease in Atrap protein in Ang II-treated mDCT cells (Fig. 1C), we examined the effect of miR-125a-5p/miR-125b-5p inhibition. To analyze this, we transfected the miR-125a-5p inhibitor into mDCT cells for 48 h, followed by treatment with Ang II for 6 h. The results showed that the miR-125a-5p inhibitor increased Atrap mRNA expression to levels similar to those induced by Ang II. No further Ang II-induced increase in Atrap mRNA was observed in the miR-125a-5p inhibitor-transfected condition (Fig. 5A). This suggested the possibility that the Ang II-induced Atrap mRNA enhancement was modulated by miR-125a-5p/miR-125b-5p. In this scenario, miR-125a-5p/miR-125b-5p needs to be repressed in the Ang II-treated condition. Consistent with this hypothesis, the

## miR-125 inhibition represses angiotensin II signaling

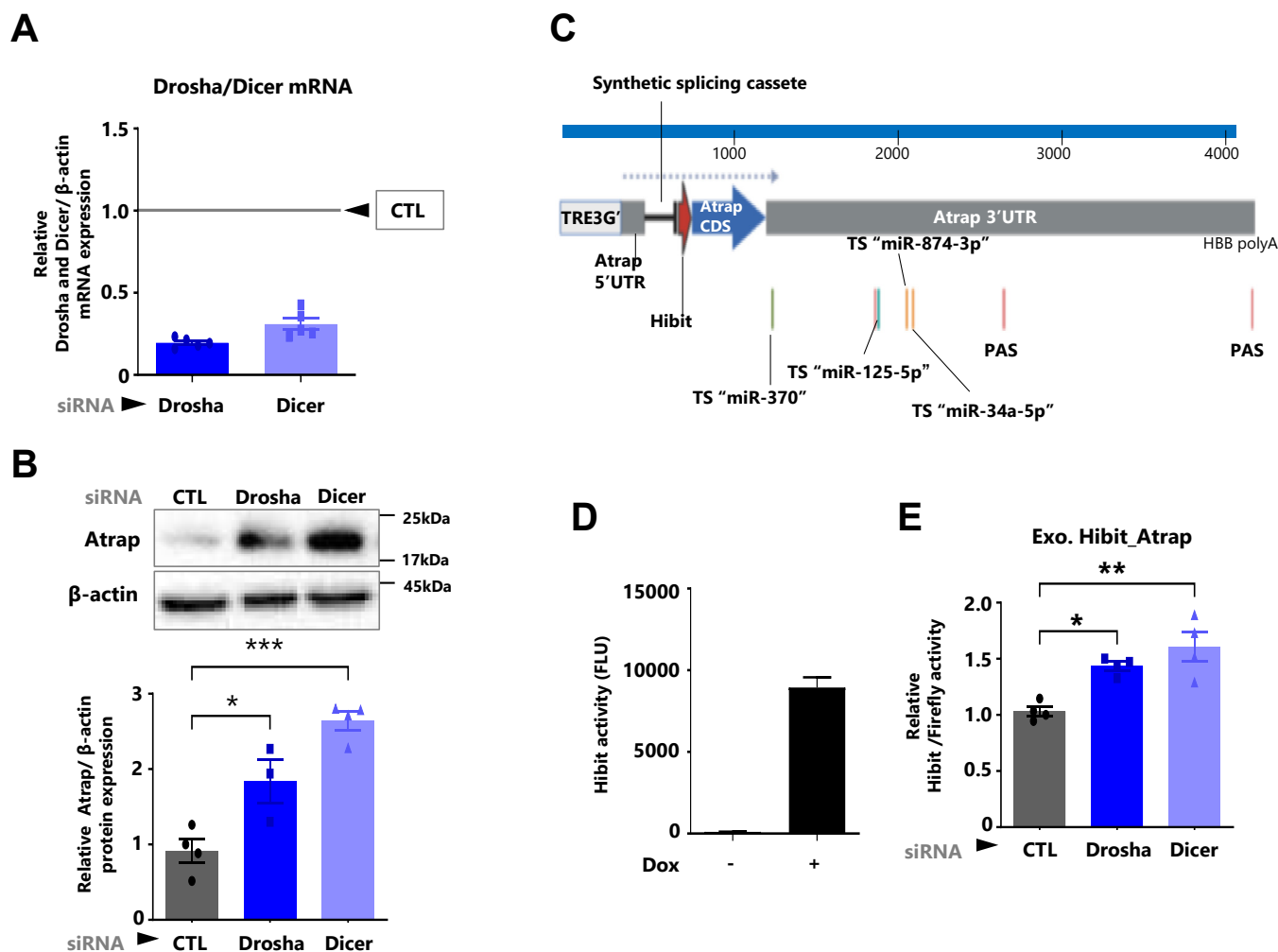


**Figure 2. miRNAs repress the expression of Atrap in mDCT cells.** Effect of the inactivation of mRNA pathway, using siRNAs of Drosha or Dicer, miRNA processing factors, and the analysis of endogenous/exogenous Atrap expression in mDCT cells. The mDCT cells were treated with negative control siRNA (control; CTL), Drosha/Dicer siRNA (Drosha/Dicer) for 48 h. *A*, confirmation of Drosha/Dicer mRNA expression by RT-qPCR, normalized to  $\beta$ -actin. The mRNA levels of the CTL group were set to 1 ( $n = 4-5$ ). *B*, the relative protein expression of Atrap in mDCT cells was determined by Western blot analysis, normalized to  $\beta$ -actin expression. The protein levels of the CTL group were set to 1 ( $n = 3-4$ ). *C* and *D*, establishment of mDCT cells capable of doxycycline (Dox)-induced Hibit-Atrap expression (schema created at [biorender.com](https://www.biorender.com)). Hibit-Atrap contains the 3' UTR sequence encompassing even the most distant poly A site (PAS). *C*, confirmation of the induction of Hibit-Atrap with Dox treatment. Hibit activity was measured by a plate reader. Hibit activity levels of the Dox group were set to 1 ( $n = 2$ ). *D*, the mDCT\_Hibit-Atrap gene cells were treated with negative control siRNA (control; CTL), Drosha/Dicer siRNA (Drosha/Dicer) for 48 h, followed with treatment by Dox for 8 h, then dual luciferase reporter assay was performed. The Hibit activity was measured by a plate reader and normalized to firefly activity. The relative Hibit/firefly levels of the CTL group were set to 1 ( $n = 4$ ). Data were obtained with three to five biologically independent experiments. Values represent the means  $\pm$  standard error. \* $p < 0.05$ , \*\* $p < 0.01$ , \*\*\* $p < 0.001$  versus siRNA-CTL group. Data were analyzed by (*B* and *E*) one-way ANOVA with Tukey's post hoc test. The data shown are presented as the mean  $\pm$  SEM. All preprocessing original Western blot data are shown in Fig. S5. Atrap, mouse Atrap; mDCT, mouse distal convoluted tubule cell; qPCR, quantitative PCR.

expression of miR-125a-5p and miR-125b-5p was found to decrease in response to Ang II treatment (Fig. 5B). These results suggested that miR-125a-5p/miR125b-5p kept decreasing Atrap mRNA under normal conditions and that Ang II stimulation repressed miR-125a-5p/miR125b-5p to promote Atrap mRNA accumulation.

### Ang II promoted Atrap protein decrease by enhancing proteasome subunit expression

As noted previously, however, Ang II treatment would decrease Atrap protein (Figs. 6, A and B, S3B, and S6). This discrepancy may reflect the alternative regulatory mechanism for the decrease in Atrap protein in response to Ang II. Two

reports described that the Ang II-induced downregulation of Atrap protein was promoted by transcriptional activation of the proteasome subunits  $\beta 5i$  and  $\beta 2i$  (Fig. 7D) (26, 27). To validate this possibility, we examined the involvement of proteolysis by the activation of the proteasome pathway using bortezomib, a protease inhibitor. The results showed that the Ang II-induced decrease in both endogenous Atrap protein and exogenous Hibit-Atrap protein was abolished by bortezomib treatment in mDCT cells (Figs. 6, C and D, S3D, and S6). Consistent with previous reports, the Ang II-stimulated upregulation of  $\beta 5i$  and  $\beta 2i$ , but not  $\beta 1i$ , proteasome subunit mRNAs was observed as putative mechanism for the decrease in Atrap protein (Figs. 7A and S4A). Enhancement of  $\beta 5i$  protein expression was confirmed by Western blotting



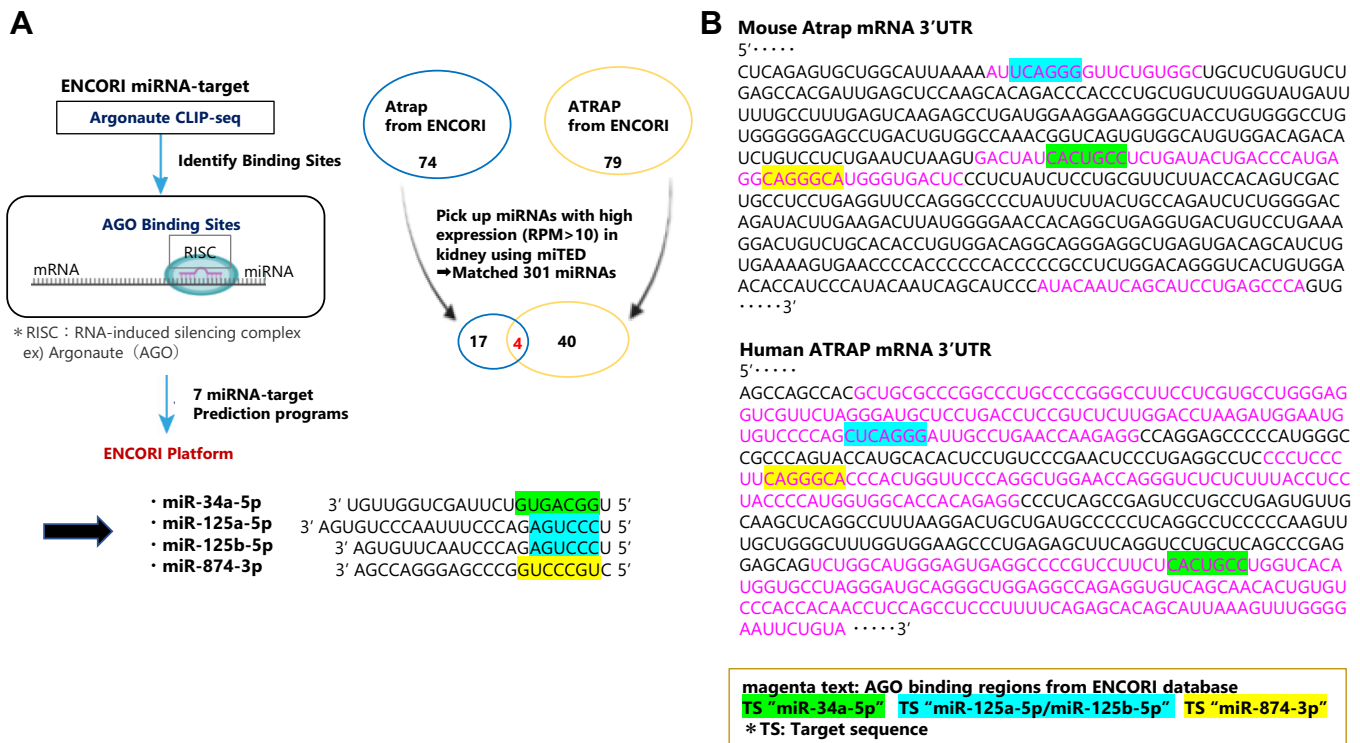


**Figure 3. Predicted the candidates of miRNA targeting *Atrap*/*ATRATP* using the database.** A, predicted the miRNAs targeting *Atrap* and *ATRATP* using ENCORI miRNA-target. ENCORI provides a comprehensive Ago2-mRNA binding dataset and includes both human and mouse genes. Then selected miRNAs with high expression (RPM > 10) in kidney using miTED. Eventually, identified four candidate miRNAs, miR-34a-5p, miR-125a-5p, miR-125b-5p, and miR-874-3p. The sequence of each miRNA is shown, and the shaded areas indicate the binding site. This figure was created using biorender.com. B, represents fragments of *Atrap* and *ATRATP* mRNA 3'UTRs. Magenta letters indicate argonaute-binding sites. The shaded areas indicate target sequences of the corresponding miRNAs. Ago2, argonaute 2; *ATRATP*, human *Atrap*; *Atrap*, mouse *Atrap*.

(Figs. 7B, S4, B and C, and S7). In contrast to miR-125a-5p/miR-125b-5p inhibition, proteasome repression did not enhance *Atrap* protein expression under normal conditions (Fig. 6C, upper panel, lanes 1 and 3; and bottom graph, columns 1 and 3; and Fig. 6D columns 1 and 3). This indicated that the proteasome degraded *Atrap* protein only in response to Ang II but not under normal conditions.

**The miR-125a-5p inhibitor and *Atrap* enhancement repressed the Ang II-stimulating expression of the proteasome subunit**

We next analyzed the involvement of miR-125a-5p/miR125b-5p in *Atrap* protein expression. Consistent with the previous results (Fig. 4), the miR-125a-5p inhibitor increased *Atrap* protein expression under normal conditions (Fig. 6A, upper panel, lanes 1 and 3; and bottom graph, columns 1 and 3). Unexpectedly, however, the miR-125a-5p inhibitor could also abolish the Ang II-induced *Atrap* protein repression (Fig. 6A, upper panel, lanes 3 and 4; and bottom graph, columns 3 and 4). The transcriptional regulation-independent effect of the miR-125a-5p inhibitor on *Atrap* protein expression was confirmed by using the Hibit-*Atrap* gene reporter, in which similar results of endogenous *Atrap* protein were observed (Fig. 6B). These results suggest that the miR-125a-5p inhibitor has the ability to suppress Ang II-induced proteasome activation.

Since Ang II stimulates the expression of proteasome subunits (Fig. 7, A–C, columns 1 and 2), we analyzed the effect of

the miR-125a-5p inhibitor on their expression. Intriguingly, the miR-125a-5p inhibitor could repress the Ang II-induced expression of proteasome subunit (Fig. 7, A and B, columns 3 and 4). This is probably through the enhancement of *Atrap* protein expression, as it could repress Ang II–AT1R signaling. To support this notion, we found that the enhancement of exogenous *Atrap* expression could also repress the Ang II-induced proteasome subunit expression (Fig. 7C, columns 3 and 4).

**The inhibition of miR-125-5p ameliorates Ang II–AT1R signaling by playing a role in regulating *Atrap* protein expression**

Finally, we examined the effect of miR-125a-5p inhibitor on other downstream effectors of Ang II–AT1R signaling; namely TGFβ mRNA (Fig. 8A), αEnaC mRNA–protein (Figs. 8, B and C, S4F, and S8), phospho-p38 (Figs. 8D, S4G, and S8), and oxidative stress (NRF2 [NFE2 like bZIP transcription factor 2] protein and HO-1 mRNA) (Figs. 8E, S4H, and S9). We showed that the Ang II stimulation enhanced all these effectors of Ang II–AT1R pathway. However, transfection of the miR-125a-5p inhibitor decreased all these downstream effectors of Ang II–AT1R signaling (Figs. 8, A–E, S4, F–H, S8, and S9). No alternation in basal level of these effectors was observed by the miR-125a-5p inhibitor, although the basal level of *Atrap* protein expression is elevated (Figs. 8, A–E, S4, F–H, S8, and S9).

## miR-125 inhibition represses angiotensin II signaling

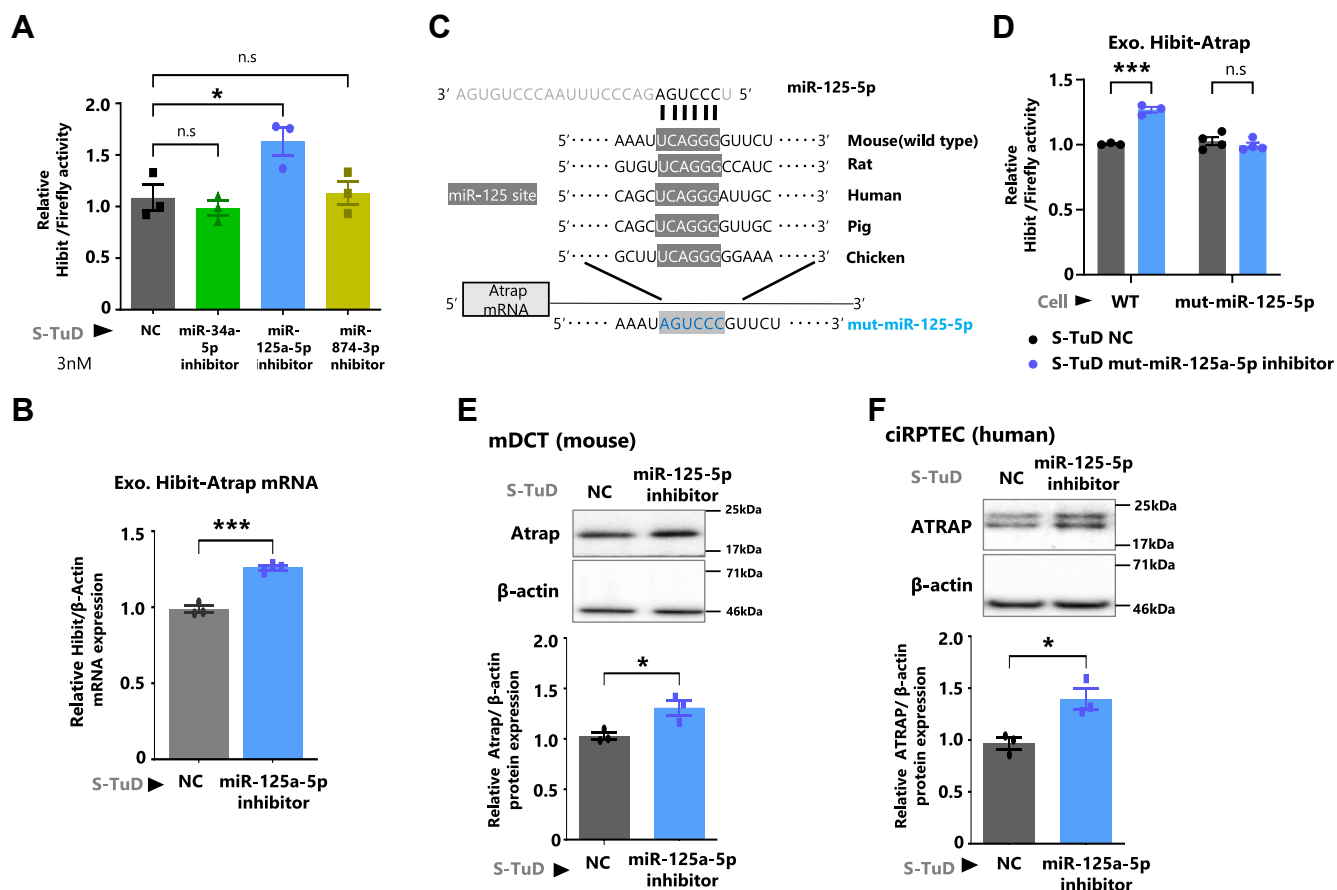


**Figure 4. Identification of miR-125-5p as an evolutionarily conserved direct repressor of Atrap-ATRAP expression.** *A*, effect of the four candidate miRNAs on Atrap mRNA, employing synthetic tough decoy (S-TuD), an miRNA inhibitor. *C* and *D*, effect of the miR-125-5p on Atrap mRNA directly, by introducing the mutation to replace a complementary sequence at the site where miR-125a-5p-miR-125b-5p can bind. *E* and *F*, effect of the miR-125-5p inhibition on endogenous Atrap-ATRAP. *A*, the mDCT\_Hibit-Atrap gene cells were treated with S-TuD (3 nM), negative control (NC), mmu-miR-34a-5p, mmu-miR-125a-5p, and mmu-miR-874-3p for 48 h, followed by the treatment with Dox for 8 h, then Dual-Luciferase Reporter Assay was performed. The Hibit activity was measured by a plate reader and normalized to firefly activity. The relative Hibit/firefly levels of the S-TuD NC group were set to 1 ( $n = 3$ ). *B*, the mDCT\_Hibit-Atrap gene cells were treated with S-TuD (3 nM), NC, and mmu-miR-125a-5p for 48 h, followed by the treatment with Dox for 8 h. The relative mRNA expression of Hibit-Atrap was determined by RT-qPCR, normalized to  $\beta$ -actin expression. The mRNA levels of the NC-CTL group were set to 1 ( $n = 3$ ). *C*, represents miR-125a-5p sequences and Atrap-ATRAP mRNA 3'UTR sequences of various species (mouse, rat, chicken, pig, and human). The shaded region indicates a possible binding sequence. The mut-miR-125-5p refers to the sequence with mutation replacing the complementary base. *D*, the mDCT\_Hibit-Atrap gene (WT) cells and the mDCT\_mut-Hibit-Atrap gene (mut-miR-125-5p) cells were treated with S-TuD (3 nM), NC, and mmu-miR-125a-5p (miR-125-5p) for 48 h, followed by the treatment with Dox for 8 h, and then Dual-Luciferase Reporter Assay was performed. The Hibit activity was measured by a plate reader and normalized to firefly activity. The relative Hibit/firefly levels of both S-TuD NC groups were set to 1 ( $n = 3$ ). *E* and *F*, the mDCT cells and human immortalized proximal tubular cells (ciRPTEC) were treated with S-TuD (3 nM), NC, and mmu-miR-125a-5p (miR-125-5p) for 48 h. The relative protein expression of Atrap-ATRAP in the mDCT cells and ciRPTEC was determined by Western blot analysis, normalized to  $\beta$ -actin expression. The protein levels of the NC group were set to 1 ( $n = 3$ ). Data were obtained with three biologically independent experiments. *A*, one-way ANOVA with Tukey's post hoc test:  $*p < 0.05$  versus NC ( $n = 3$ ). *B*, an unpaired *t* test:  $*p < 0.05$  versus S-TuD NC ( $n = 3$ ). The data shown are presented as the mean  $\pm$  SEM. *D*, values represent the means  $\pm$  standard error.  $***p < 0.001$  versus CTL group. Data were analyzed by two-way ANOVA with Tukey's post-hoc test,  $n = 3$  to 4. The data shown are presented as the mean  $\pm$  SEM. *E* and *F*, values represent the means  $\pm$  standard error.  $*p < 0.05$  versus NC group. Data were analyzed by unpaired *t* test,  $n = 3$ . The data shown are presented as the mean  $\pm$  SEM. All preprocessing original Western blot data are shown in Fig. S5. ATRAP, human ATRAP; Atrap, mouse Atrap; CTL, control; Dox, doxycycline; mDCT, mouse distal convoluted tubule cell; qPCR, quantitative PCR.

$\gamma$ ENaC protein (non-Ang II effector) showed no significant change neither by Ang II treatment nor by the treatment with miR-125a-5p inhibitor (Figs. 8C, S4F, and S8). These results showed that miR-125a-5p/miR-125b-5p inhibition not only enhanced Atrap protein expression but also decreased the Ang II-AT1R signaling pathway.

### Discussion

In the present study, we demonstrated that miR-125a-5p/miR-125b-5p directly acts on Atrap/ATRAP mRNA and represses its expression in mouse distal tubular cells, mDCT, and

human proximal tubular epithelial cells, ciRPTEC. In addition, we found that miR-125a-5p/miR-125b-5p inhibition attenuated the proteasome-mediated decrease in Atrap protein expression in response to Ang II treatment. Furthermore, we revealed that miR-125a-5p-miR-125b-5p inhibition antagonized the effects of Ang II inducing cellular responses consisting of the proteasome subunits, TGF $\beta$  and  $\alpha$ ENaC expression, and p38 mitogen-activated protein kinase activation in mDCT cells. These results suggest that miR-125a-5p/miR-125b-5p promotes the Ang II-AT1R signaling and may be involved in the pathogenesis of hypertension and cardiovascular disease.

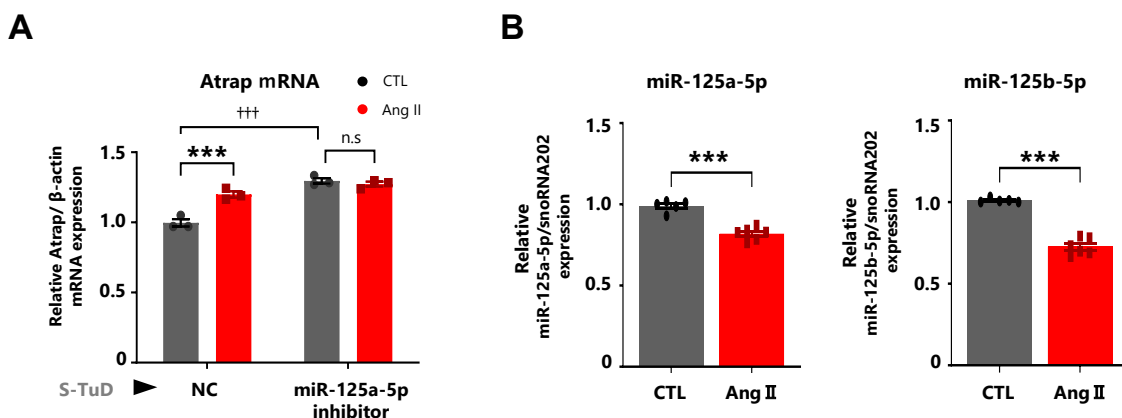


**Figure 5. Ang II promoted Atrap mRNA accumulation by repressing miR-125a-5p–miR125b-5p expression.** Effect of the miR-125-5p inhibition on Atrap mRNA in Ang II-stimulated mDCT cells. *A*, the relative mRNA expression of Atrap was determined by RT–qPCR, normalized to  $\beta$ -actin expression. The mRNA levels of the NC–CTL group were set to 1 ( $n = 3$ ). *B*, the mDCT\_Hibit-Atrap gene cells were treated with 1  $\mu$ M Ang II for 6 h. The relative miRNA expression of miR-125a-5p and miR-125b-5p was determined by RT–qPCR analysis, normalized to snoRNA202 expression. The miRNA levels of the CTL group were set to 1 ( $n = 5$ –6). \* $p < 0.05$ , \*\* $p < 0.01$ , \*\*\* $p < 0.001$  versus CTL. †† $p < 0.01$ , ††† $p < 0.001$  versus NC–CTL. Data were obtained with three (*A*) or five to six (*B*) biologically independent experiments. Data were analyzed by (*A*) two-way ANOVA with Tukey's post hoc test and (*B*) unpaired  $t$  test. The data shown are presented as the mean  $\pm$  SEM. Ang II, angiotensin II; Atrap, mouse Atrap; CTL, control; mDCT, mouse distal convoluted tubule cell; NC, negative control; qPCR, quantitative PCR.

Consistently, a previous report presented that miR-125b-5p was identified as the driver of Ang II–TGF $\beta$  profibrotic signaling (37). In this report, the locked nucleic acid–based inhibition of miR-125b-5p was found to protect the Ang II infusion inducing cardiac fibrosis in mice. The authors showed that the Ang II infusion enhances miR-125b-5p expression through TGF $\beta$  signaling in the mouse heart. Furthermore, our group previously reported that Ang II infusion decreases Atrap mRNA and Atrap protein expression in the heart and outer renal medulla of mice (19, 44). On the other hand, in the present study, we showed that the Ang II treatment immediately decreased the expression of miR-125a-5p and miR-125b-5p in mDCT cells (Fig. 5B). The expression of miR-125a-5p/miR-125b-5p may vary because of time-dependent modulation, where primary Ang II signaling represses and secondary TGF $\beta$  signaling restores/promotes their expression, causing discrepancies in the effects on tissues and mDCT cells. Consistent with this view, TGF $\beta$  induces the transcriptional activation of the miR-125b-1 host gene (45). TGF $\beta$ –receptor expression may vary among cells/tissues, and therefore, the effect of Ang II stimulation on miR-125a-5p/miR-125b-5p expression would be different. Nevertheless, it remains coherent that the inhibition of miR-125a-5p and miR-125b-5p effectively suppresses Ang II-induced pathological responses in both the heart and kidney. Therefore, miR-125a-5p/miR-125b-5p could be a therapeutic target for hypertension and cardiac fibrosis.

Wang *et al.* (46) proposed that the Ang II-induced enhancement of proteasome subunits is prerequisite to reduce Atrap expression in a mouse model. In line with this, our study demonstrated that the degradation of Atrap protein in mDCT cells by Ang II stimulation was mediated by the activation of proteasome subunits. This mechanism could be explained by our results in which the miR-125a-5p inhibitor caused the enhancement of exogenous Atrap expression or the increase in endogenous Atrap expression, thereby preventing

the Ang II–AT1R signaling–mediated proteasome subunit expression (Fig. 7D).

On the other hand, we found that the miR-125a-5p inhibitors also upregulated ATRAP expression in human ciRP-TEC cells (Fig. 4F). However, we were unable to analyze the effects of Ang II stimulation for ATRAP expression because of the faint Ang II response in our ciRPTEC cells. This is one of the limitations of our current work. We need to develop human cells that can respond to the Ang II stimulation. Alternative regulatory mechanisms may promote the decrease of ATRAP expression in human Ang II-associated pathologies (25) because the lysine residues of the Atrap ubiquitination site are missing in human ATRAP (Fig. S2F). Therefore, it is desirable to further investigate the role of the miR-125 family under Ang II stimulation in human tissues and cells.

We also observed that the miR-125a-5p inhibitor suppressed the activation of proteasome subunits (Fig. 7, A and B) and the degradation of Atrap protein (Fig. 5, A and B). However, miRNAs have multiple targets in a single signaling process (47). Therefore, our results may not be solely because of the increased Atrap expression. Although our study did not include an *in vivo* examination, such an analysis would be valuable to predict off-target effects for *in vivo* administration. In addition, it would be important to know the precise target organs/tissues for delivery of miR-125a-5p/miR-125b-5p inhibitor consisting of antisense locked nucleic acid or S-TuD to enhance its potential as a therapeutic target.

We showed that the Ang II treatment enhanced Atrap mRNA expression most likely through the decrease of miR-125a-5p/miR-125b-5p. This enhancement may be one of the feedback regulation mechanisms of Atrap protein abundance. In this case, Atrap protein would rapidly recover after Ang II ablations to suppress the pathogenic/excessive activation of Ang II–AT1R signaling (48). In addition to the post-transcriptional regulation of Atrap expression described in the present study, Atrap expression can also be

## miR-125 inhibition represses angiotensin II signaling

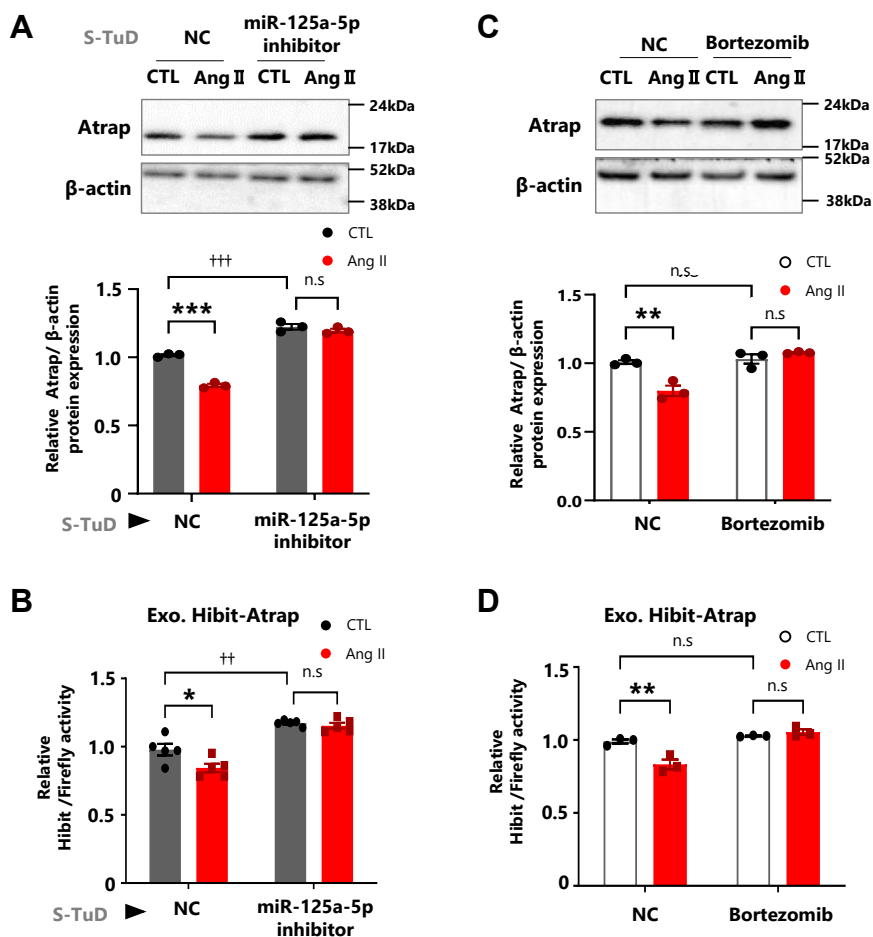


**Figure 6. Ang II enhanced proteasome subunit expression, reducing Atrap protein.** A and B, effect of the miR-125-5p inhibition on Atrap mRNA in Ang II-stimulated mDCT cells. C and D, effects of the Ang II and bortezomib treatment on Atrap degradation in mDCT cells. A, the mDCT\_Hibit-Atrap gene cells were treated with S-TuD (3 nM), negative control (NC), and mmu-miR-125a-5p (miR-125-5p) for 48 h, followed by the treatment with 1  $\mu$ M Ang II for 6 h. The relative protein expression of Atrap was determined by the Western blot analysis, normalized to  $\beta$ -actin expression. The protein levels of the NC-CTL group were set to 1 (n = 3). B, the mDCT\_Hibit-Atrap gene cells were treated with S-TuD (3 nM), NC, and mmu-miR-125a-5p (miR-125-5p) for 48 h, and then Dual-Luciferase Reporter Assay was performed after treatment with Dox and Ang II. Hibit activity was measured by a plate reader and normalized to firefly activity. The relative Hibit/firefly levels of the NC-CTL group were set to 1 (n = 5). C, the relative protein expression of Atrap, after 6 h of treatment with 1  $\mu$ M Ang II and/or 10 nM bortezomib, was determined by Western blot analysis, normalized to  $\beta$ -actin expression. The protein levels of the NC-CTL group were set to 1 (n = 3). D, Dual-Luciferase Reporter Assay was performed after treatment with Dox and Ang II-bortezomib for 6 h. The Hibit activity was measured by a plate reader and normalized to firefly activity. The relative Hibit/firefly levels of NC-CTL group was set to 1 (n = 3). \* $p < 0.05$ , \*\* $p < 0.01$ , \*\*\* $p < 0.001$  versus CTL. <sup>†</sup> $p < 0.05$  versus NC-CTL. Data were obtained with three (A, C, and D) or five (B) biologically independent experiments. Data were analyzed by two-way ANOVA with Tukey's post hoc test. The data shown here are presented as the mean  $\pm$  SEM. All preprocessing original Western blot data are shown in Fig. S6. Ang II, angiotensin II; Atrap, mouse Atrap; CTL, control; Dox, doxycycline; mDCT, mouse distal convoluted tubule cell; S-TuD, synthetic tough decoy.

transcriptionally regulated by Runx3 and USF1/USF2 (20, 49). Further analysis including these factors will help to understand the more precise regulatory mechanism of Atrap under Ang II-stimulated conditions.

The involvement of Ang II-AT1R signaling in the development and progression of nonalcoholic fatty liver disease and cancer has been well documented (50, 51). In the context of nonalcoholic fatty liver disease, ATRAP protein expression is decreased (22), whereas miR-125b-5p is upregulated (52). On the other hand, ATRAP expression is upregulated in various cancers, including bladder urothelial carcinoma, breast invasive carcinoma, hepatocellular carcinoma, lung adenocarcinoma, kidney cancer, and multiple gastrointestinal cancers (23). Intriguingly, the expression level of miR-125a-5p and/or miR-125b-5p is decreased in bladder urothelial carcinoma, breast cancer, hepatocellular carcinoma, colorectal cancer, cervical cancer, and lung adenocarcinoma (53–58). Although

the expression of the miR-125 family and ATRAP is negatively correlated, the direct relationship between them in these diseases remains unknown. Further investigation holds the potential to define new therapeutic targets.

In conclusion, our findings show that the miR-125a-5p/miR-125b-5p not only directly represses Atrap-ATRAP expression in renal tubular cells but also promotes Ang II-AT1R activation. These results suggest new avenues for potential therapeutic approaches to achieve the organ-protective effects of the miR-125a-5p/miR-125b-5p inhibitor in Ang II-associated diseases.

## Experimental procedures

### Cell culture

The mDCT cells were kindly provided by Dr Peter A. Friedman (University of Pittsburgh School of Medicine). These



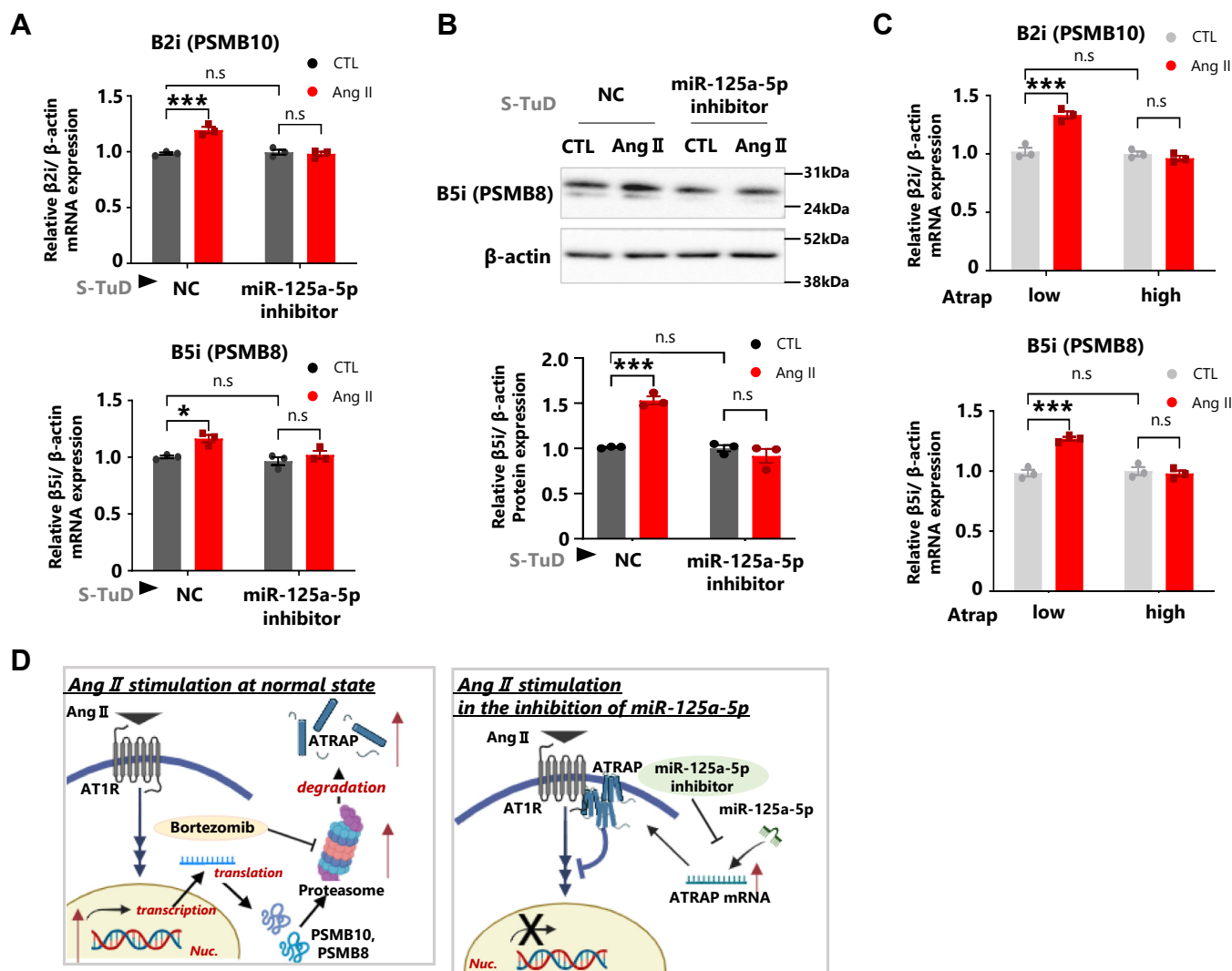


**Figure 7. Atrp upregulation and miR-125a-5p inhibition suppressed proteasome subunit expression stimulated by Ang II.** A and B, effect of the miR-125-5p inhibition on Atrap mRNA in Ang II-stimulated mDCT cells. C, effects of the enhancing exogenous Atrap expression for the Ang II-induced proteasome subunit expression. A, the relative mRNA expression of  $\beta 2i$  and  $\beta 5i$  was determined by RT-qPCR, normalized to  $\beta$ -actin expression. The mRNA levels of the NC-CTL group were set to 1 ( $n = 3$ ). B, the relative protein expression of  $\beta 5i$  was determined by Western blot analysis, normalized to  $\beta$ -actin expression. The protein levels of the NC-CTL group were set to 1 ( $n = 3$ ). C, the mDCT\_Hibit-Atrap gene cells were treated with/without 3  $\mu$ g Dox for 24 h, and then 1  $\mu$ M Ang II was added for 6 h. The relative mRNA expression of  $\beta 2i$  and  $\beta 5i$  was determined by RT-qPCR, normalized to  $\beta$ -actin expression. The mRNA levels of the Dox (-)-CTL group were set to 1 ( $n = 3$ ). D, a schematic diagram of Ang II-AT1R-proteasome pathway in our analysis, which was created at [biorender.com](https://www.biorender.com). \* $p < 0.05$ , \*\* $p < 0.01$ , \*\*\* $p < 0.001$  versus CTL. <sup>†</sup> $p < 0.05$  versus NC-CTL. Data were obtained with three biologically independent experiments. Data were analyzed by two-way ANOVA with Tukey's post hoc test. The data shown here are presented as the mean  $\pm$  SEM. All preprocessing original Western blot data are shown in Fig. S7. Ang II, angiotensin II; Atrap, mouse Atrap; CTL, control; Dox, doxycycline; mDCT, mouse distal convoluted tubule cell; NC, negative control; qPCR, quantitative PCR.

cells have been shown to have a phenotype of a polarized tight junction epithelium along with both morphological and functional features retained from the parental cells (59). The mDCT cells were cloned with limiting dilution, resulting in the isolation of six individual clones. These cloned mDCT cells, along with other noncloned mDCT cells, were maintained in Dulbecco's modified Eagle's medium (DMEM)/Ham's F12 medium supplemented with 5% fetal bovine serum (FBS) (Sigma-Aldrich) in a CO<sub>2</sub> incubator.

The normal human RPTECs were purchased from Lonza (catalog no.: CLCC-2553, lot no.: 0000203150, Caucasian female, 10 years old) and immortalized by infecting it with lentivirus-expressing human telomerase reverse transcriptase

and shRNA targeting p16 (plenti6\_TERT\_sh-p16). The immortalized RPTECs (ciRPTECs) were cloned as mentioned previously (24). The ciRPTECs were cultured in DMEM with 10% FBS in a CO<sub>2</sub> incubator.

#### Isolation of genomic DNA and cloning the complementary DNA of Atrap including the 3'UTR region

Mouse genomic DNA was extracted from mDCT cells. The Wizard Genomic DNA Purification Kit from Promega was used for this purpose, according to the manufacturer's instructions. The extracted DNA samples were then used as templates for PCR amplification of the target genes, specifically

## miR-125 inhibition represses angiotensin II signaling

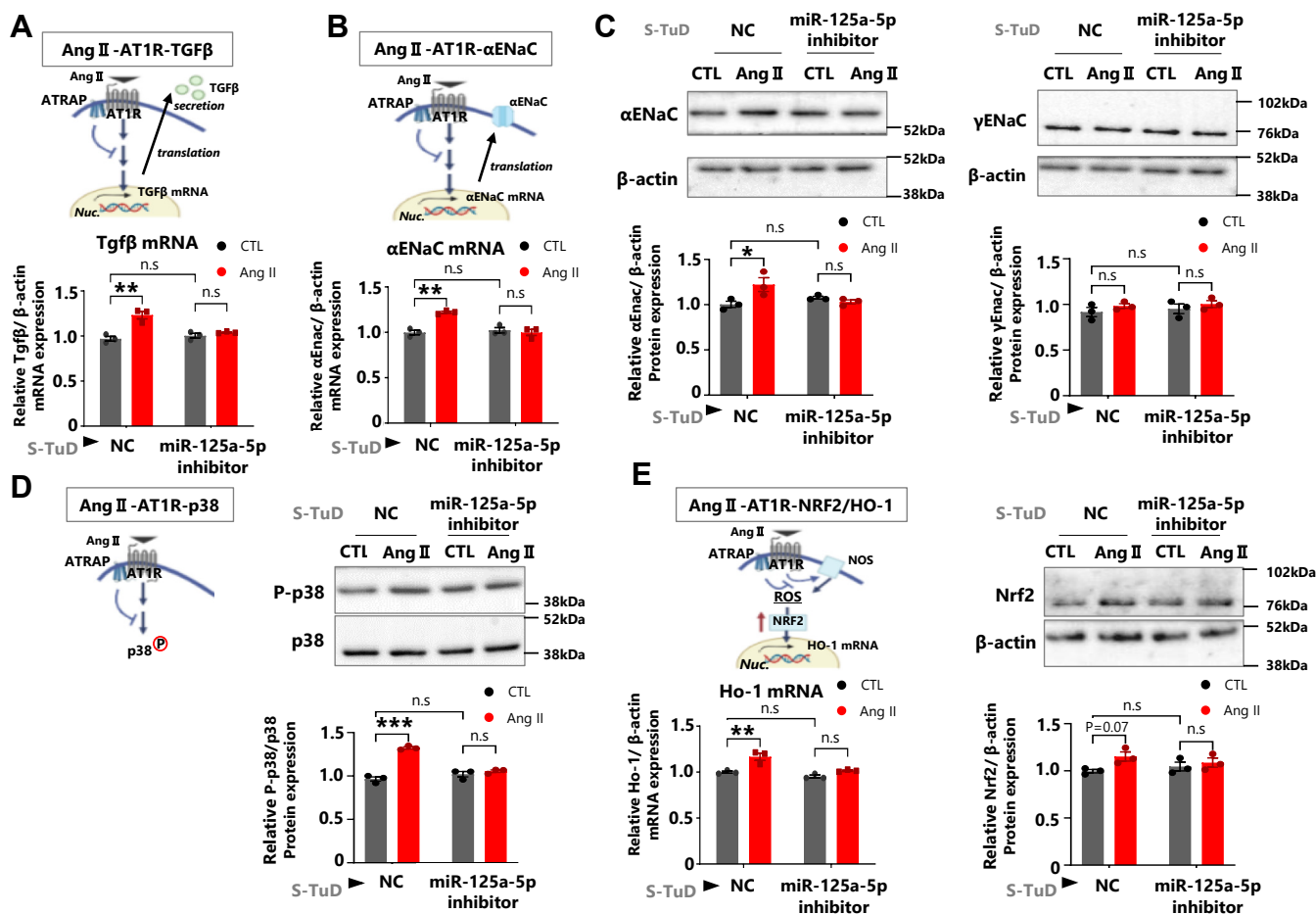


**Figure 8. The inhibition of miR-125-5p ameliorates Ang II-AT1R signaling by playing a role in regulating Atrap protein expression.** Effect of the miR-125-5p inhibition in response to various Ang II-AT1R signaling pathways in mDCT cells. *A*, upper, schematic diagram of Ang II-AT1R-TGF $\beta$  pathway in our analysis. Lower, the relative mRNA expression of Tgf $\beta$  as determined by RT-qPCR, normalized to  $\beta$ -actin expression. The mRNA levels of the NC-CTL group were set to 1 ( $n = 3$ ). *B*, upper, schematic diagram of Ang II-AT1R- $\alpha$ ENaC pathway in our analysis. Lower, the relative mRNA expression of  $\alpha$ ENaC was determined by RT-qPCR, normalized to  $\beta$ -actin expression. The mRNA levels of the NC-CTL group were set to 1 ( $n = 3$ ). *C*, the relative protein expression of  $\alpha$ / $\gamma$ ENaC was determined by Western blot analysis, normalized to  $\beta$ -actin expression. The Western blot data of  $\beta$ -actin were the same as in Fig. 5B (left panel) and Figure 6A (right panel). The protein levels of the NC-CTL group were set to 1 ( $n = 3$ ). *D*, upper, schematic diagram of Ang II-AT1R-p38 pathway in our analysis. Lower, the relative protein expression of p-p38 was determined by Western blot analysis, normalized to p38 expression. The protein levels of the NC-CTL group were set to 1 ( $n = 3$ ). *E*, upper, schematic diagram of Ang II-AT1R-NRF2/HO-1 pathway in our analysis. Lower, the relative protein expression of Nrf2 was determined by Western blot analysis, and the relative mRNA expression of HO-1 was determined by RT-qPCR, normalized to  $\beta$ -actin expression. The mRNA and protein levels of the NC-CTL group were set to 1 ( $n = 3$ ). \* $p < 0.05$ , \*\* $p < 0.01$ , \*\*\* $p < 0.001$  versus CTL. † $p < 0.05$  versus NC-CTL. Data were obtained with three biologically independent experiments. Data were analyzed by two-way ANOVA with Tukey's post hoc test. The data shown are presented as the mean  $\pm$  SEM. All preprocessing original Western blot data are shown in Figs S8 and S9.  $\alpha$ ENaC, alpha epithelial sodium channel; Ang II, angiotensin II; AT1R, Ang II type 1 receptor; Atrap, mouse ATRap; CTL, control; HO-1, heme oxygenase 1; mDCT, mouse distal convoluted tubule cell; NC, negative control; NRF2, NFE2 like bZIP transcription factor 2; qPCR, quantitative PCR; TGF $\beta$ , transforming growth factor beta.

the Atrap gene with its 3' UTR. The following primers were used: Atrap (forward: 5'-AGCTCTGTGAGCRRGTGGTC-3', reverse: 5'-TAAAGGTGCCCTCCCTCAGGA-3').

### Predicted miRNAs targeting Atrap-ATRAP

To identify evolutionarily conserved miRNAs targeting Atrap-ATRAP mRNA, we employed two databases: ENCORI (40) and miTED (41). miRNAs typically act in the site where RNA-induced silencing complex, such as Argonaute1-4 (Ago1-4), binds to the target gene mRNAs. ENCORI provides a comprehensive Ago2-mRNA binding dataset (Fig. 3A) and includes both human and mouse genes. On the other hand, miTED provides valuable information on miRNA expression levels in various human tissues and cell lines. As a result, we

identified four candidates according to the algorithm in Figure 3A.

### Establishment of mDCT cells capable of Dox-induced Hibit-mouse Atrap gene expression

In this study, we constructed three plasmids: pLenti\_TetOn\_Hibit-Atrap gene (Hibit-Atrap gene, containing blasticidin-resistance gene), mutation-miR-125-5p\_binding\_site-Hibit-Atrap gene (mut-miR-125-Hibit-Atrap gene, containing blasticidin-resistance gene), and pLenti\_SV40p-Luc2 (SV40-Luc2, containing puromycin-resistance gene) plasmids. Dox was used to induce Hibit-Atrap based on the Tet-On system. The Hibit tag was inserted at the 5'-terminal region of the Atrap coding sequence.

Detailed plasmid maps are available upon request. Lentiviral supernatants were produced as described elsewhere. Briefly, pLenti\_TetOn\_Hibit-Atrap gene (including mutant plasmid) or pLenti\_SV40p-Luc2 (3 µg), pLP1, 3 µg of pLP2/VSVG (3 µg; Thermo Fisher Scientific), and pAdvantage (1.3 µg; Promega) were mixed in Opti-MEM medium (1.5 ml; Thermo Fisher Scientific) and added to Lipofectamine 2000 (39.9 µl; Thermo Fisher Scientific) in Opti-MEM (1.5 ml). The resulting solution was mixed and incubated for 20 min at room temperature. While incubating the DNA–Lipofectamine mixture, LentiX human embryonic kidney 293T cells (Thermo Fisher Scientific) ( $5 \times 10^6$ ) were seeded in a poly-L-lysine-coated 10 cm tissue culture plate. After the incubation, the DNA–Lipofectamine mixtures were added to the LentiX human embryonic kidney 293T cells. At 8 h post-transfection, the medium was exchanged with DMEM containing 10% FBS and 10 µM forskolin. After 24~48 h, the culture supernatants were collected and filtered through 0.22 µm Steriflip filters (Millipore) to generate the lentiviral supernatants. For the lentiviral infections, the lentiviral supernatant (2 ml) was incubated with mDCT cells or Hibit-Atrap gene (including mutant plasmid) mDCT ( $1.0 \times 10^6$ ) for 24 h. Thereafter, the lentiviral supernatants were discarded followed by the addition of DMEM/Ham's F12 containing blasticidin (1.5 µg/ml) or puromycin (2.5 µg/ml). Finally, we stably cotransfected the mDCT cells with a plasmid expressing Hibit-Atrap and Luc2. The Hibit tag served as a NanoLuc reporter to Atrap protein expression, and Luc2 was also employed as a firefly luciferase to measure cellular internal standards, which allowed the use of the Dual-Luciferase Reporter Assay system.

#### siRNA and cell transfection

The following siRNAs purchased from Qiagen were used: Droscha siRNA #1: (Mm\_Etohi2\_1 FlexiTube siRNA), Dicer siRNA #1: (Mm\_Dicer1\_1 FlexiTube siRNA) and AllStars negative control siRNA.

The mDCT cells were seeded in 12-well plates and transfected with Lipofectamine RNAiMax Reagent (Thermo Fisher Scientific) for 48 h at 37 °C according to the manufacturer's protocol.

#### miRNA inhibitor assay (S-TuD assay)

The S-TuD were obtained from Ajinomoto Bio-Pharma, including mmu-miR-34a-5p, mmu-miR-125a-5p, mmu-miR-874-3p, and a negative control.

Transfection of the S-TuD into mDCT cells/ciRPTEC was performed in a 12-well plate, seeded at a density of  $5 \times 10^4/1 \times 10^5$  cells per well and transfected with 75 µl of OptiMEM, 1 µl of Lipofectamine 2000 Reagent, and 1 or 3 µl of the respective S-TuD (mmu-miR-34a-5p, mmu-miR-125a-5p, mmu-miR-874-3p, or negative control). S-TuD was prepared at a concentration of 1 µM, and the final concentration used for transfection was 1 to 3 nM. After 48 h of incubation, S-TuD-treated cells were used in subsequent experiments.

#### Dual-Luciferase Reporter Assay

The mDCT\_Hibit-Atrap gene cells transfected with each S-TuD were seeded into a 96-well plate containing 100 µl of DMEM/Ham's F12 medium supplemented with 5% FBS. The cells were treated with or without Dox (3 µg/ml) and incubated for 4~8 h. After incubation, half of the medium was removed from each well, and 50 µl of ONE-Glo EX Luciferase Assay Buffer (Promega) was added. The reaction was allowed to occur at room temperature for 10 min. Luminescence measurement was performed to quantify the Luc2 (firefly luciferase) signal using a plate reader. Subsequently, 50 µl of NanoDLR Stop & Glo Buffer containing 1% NanoDLR Stop & Glo Substrate and 1% Lgbit Protein was added to each well. Then again, the plate was incubated for 10 min at room temperature to allow the reaction. Luminescence measurement was performed to quantify the NanoLuc (Hibit + Lgbit) signal using a plate reader. This experimental setup helped to determine the quantification of Hibit-Atrap expression using the NanoLuc reporter (Hibit) and normalization with the internal standard Luc2 (firefly luciferase).

#### Western blot analysis

Western blot analysis was performed as described elsewhere (60). Briefly, total protein was extracted from cells using a sample buffer containing SDS (1%). Then, the protein concentration in each sample was measured with a Qubit 2.0 Fluorometer (Thermo Fisher Scientific). An equal amount of each protein extract was resolved on a 5 to 20% polyacrylamide gel (ATTO Corporation) and electrophoresed. After separation, the proteins were transferred to a polyvinylidene fluoride membrane. The membranes were blocked for over 1 h at room temperature with Tris-buffered saline with Tween containing skim milk (5%) or Blocking One-P (nacalai tesque) and probed overnight at 4 °C with specific primary antibodies. Antibodies against the following proteins were used: Atrap and ATRAP (1:1000–3000 dilution, rabbit, developed in our previous study (60)), β-actin (1:5000 dilution, catalog no.: A5441, mouse, Sigma–Aldrich), β5 (PSMB5) (1:10,000 dilution, catalog no.: 19178-1-AP, rabbit, Proteintech), β5i (PSMB8) (1:1000 dilution, catalog no.: 13635, rabbit, CST), αENaC (1:1000 dilution, PA1-920A, rabbit, Invitrogen), γENaC (1:2000 dilution, catalog no.: ab3468, rabbit, abcam), active p38 (1:3000 dilution, catalog no.: V121A, rabbit, Promega), p38 (1:1000 dilution, N-20, rabbit, Santa Cruz), and Nrf2 (1:2000 dilution, catalog no.: GTX103322, rabbit, GeneTex). The membranes were washed and further incubated with an appropriate secondary antibody for 60 min at room temperature. When detecting Atrap–ATRAP, αENaC, γENaC and p38, anti-Rabbit immunoglobulin G (IgG), horseradish peroxidase (HRP)-Linked Whole Ab (NA934-1Ml, donkey, GE Healthcare), was diluted 1:2000 to 5000 with Tris-buffered saline with Tween containing skim milk (5%). When detecting β-actin, antimouse IgG, HRP-Linked Whole Ab (NA931-1Ml, sheep, GE Healthcare) was diluted 1:5000. When detecting Active p38, anti-Rabbit IgG, HRP-Linked Whole Ab (NA934-1Ml, donkey, GE Healthcare), was diluted 1:5000 with Signal Enhancer Hikari solution B



## miR-125 inhibition represses angiotensin II signaling

(nacalai tesque). Full-range Rainbow Molecular Weight Markers (Cytiva) (Figs. 6, A and C, 7B, 8, C–E, S3, B and D, and S4, B, C, F, G, and H) and DynaMarker protein MultiColor Ladder Marker (Figs. 1D, 2B, 4, E and F, S1E, and S2, A, E, and F), stable II were used as molecular weight markers. The bands were visualized using Luminata Classico/Forte (Merck) or ImmunoStar LD (Fujifilm Wako Pure Chemical) as the enhanced chemiluminescence substrate. The resulting images were quantitatively analyzed using a Chemidoc Touch Imager (Bio-Rad Laboratories). All these experiments were performed at least three times, and representative results are illustrated.

### RT-qPCR analysis

Total RNA was extracted from mDCT cells using the NucleoSpin RNA Plus Kit (Takara Bio) or MagMAX mirVana Total RNA Isolation Kit (Thermo Fisher Scientific), and complementary DNA was produced using ReverTra Ace qPCR RT Master Mix with genomic DNA Remover (Toyobo) and TaqMan MicroRNA Reverse Transcription Kit (Thermo Fisher Scientific). RT-qPCR was performed with a Bio-Rad CFX96 Touch Real-Time PCR Detection System (Bio-Rad Laboratories), and the reverse-transcribed products were incubated with THUNDERBIRD Next SYBR qPCR Mix (Toyobo) or TaqMan Fast Advanced Master Mix (Thermo Fisher Scientific). The Atrap-Ho-1 mRNA levels were normalized to those of  $\beta$ -actin. The miR-125a-5p and miR-125b-5p miRNA levels were normalized to those of snoRNA202.

The following primers were used: Atrap (forward: 5'-CC ACCATCTTCTGGACATT-3', reverse: 5'-AGACGAGGCA GCAAGAGAAG-3'), Drosha (forward: 5'-GGACCATCAC-GAAGGACACT-3', reverse: 5'-CACGGGTCTCTTGGTTT TGT-3'), Dicer (forward: 5'-ACCAAGTGATCCGTTTACGC-3', reverse: 5'-CAACCGTACACTGTCCATCG-3'),  $\beta$ -actin (forward: 5'-GCCGCCAGCTCACCAT-3', reverse: 5'-TCGT CGCCACATAGGAATC-3'), Scnn1a ( $\alpha$ ENaC): (forward: 5'-ACCCCGTGAGTCTCAACATC-3', reverse: 5'-CCTGGCGA GTGTAGGAAGAG-3'), Tgf- $\beta$  (forward: 5'-TGCTTCAGCT CCACAGAGAA-3', reverse: 5'-TGGTTGTAGAGGGCAAG GAC-3'), Cdh1 (cadherin; forward: 5'-AGCCATTGCCAAG-TACATCC-3', reverse: 5'-AAAGACCGGCTGGGTAAACT-3'), Cdh2 (forward: 5'-AGGGTGGACGTCATTGTAGC-3', reverse: 5'-CTGTTGGGGTCTGTCAGGAT-3'), Calb1 (calbindin 1; forward: 5'-CCACCTGCAGTCATCTCTGA-3', reverse: 5'-TTCCGGTGATAGCTCCAATC-3'), Aqp2 (aquaporin 2; forward: 5'-TTGCCATGTCTCCTTCTTC-3', reverse: 5'-GGTCAGGAAGAGCTCCACAG-3'), Ncc (sodium-chloride cotransporter; forward: 5'-CTGGAGAACCTGTTGCTTC-3', reverse: 5'-GATGTCACCATGACCGACAG-3'), Pth1r (parathyroid hormone 1rReceptor; forward: 5'-ATCTTCGTGAAG-GACGCTGT-3', reverse: 5'-CCCTCCACCAGAATCCAGTA-3'), At1r (forward: 5'-GGAAACAGCTTGGTGGTGAT-3', reverse: 5'-ACATAGGTGATTGCCGAAGG-3'), Hibit-Atrap (forward: 5'-AGAAGATCAGCGGAGAGCTG-3', reverse: 5'-GGCCAGGATAGTGAAGTTGC-3'),  $\beta$ 1i (PSMB9) (forward: 5'-TCTTCTGTGCCCTCTCAGGT-3', reverse: 5'-GGTCCC AGCCAGCTACTATG-3'),  $\beta$ 2i (PSMB10) (forward: 5'-

CTTTACTGCCCTTGGCTCTG-3', reverse: 5'-GTGATCACA CAGGCATCCAC-3'),  $\beta$ 5i (PSMB8) (forward: 5'-CAGTCCT-GAAGAGGCTACG-3', reverse: 5'-CACTTTCACCCAACC GTCTT-3'), and Ho-1 (forward: 5'-TTGAGGAGCTGCA GGTGATG-3', reverse: 5'-TGCCAACAGGAAGCTGAGAG-3'). For the detection of miRNA expression, we purchased TaqMan MicroRNA Assay (has-miR-125a-5p, has-miR-125b-5p, and snoRNA202) from Thermo Fisher Scientific.

### Statistical analysis

Statistical analyses were performed with GraphPad Prism9 (GraphPad Software). All data are shown as the mean  $\pm$  SEM. Differences were analyzed using the following statistical tests. Two-way ANOVA, followed by Tukey's post hoc analysis, was performed to determine differences between CTL (control) and Ang II groups (Figs. 5, A–C, 6, 7, 8, and S4, A, B, and D). One-way ANOVA, followed by Tukey's post hoc analysis, was performed to determine differences between CTL and other groups (Figs. 2, B and E, and 4A). In addition, an unpaired *t* test was used to analyze the differences between the two groups (Figs. 1, B–D, 4, B, E, and F, and 5D). *p* Values <0.05 were considered statistically significant. Data were obtained with three to five biologically independent experiments.

### Data availability

The data presented in this study are available on request from the corresponding author.

**Supporting information**—This article contains supporting information (10, 15, 38, 59).

**Acknowledgments**—We express our gratitude to K. Aoyagi (Yokohama City University) for the help with the experiments. We would also thank Ms Naima Batool for editing the English grammar of the article. Finally, we would like to express regard to Dr Yumiko Fujikawa for the critical reading/proofreading of the article. The project received supports from grants provided by the Yokohama Foundation for Advancement of Medical Science; the Uehara Memorial Foundation; the Japan Society for the Promotion of Science; the Japan Kidney Association-Nippon Boehringer Ingelheim Joint Research Program; the Japanese Association of Dialysis Physicians; the Strategic Research Project of Yokohama City University; and the Moriya Scholarship Foundation. Science and Technology Agency (JST) (Moonshot R&D).

**Author contributions**—A. Y. and K. T, conceptualization; K. H. validation; K. H., E. A., T. Y., Shohei Tanaka, Shinya Taguchi, and Shunichiro Tsukamoto formal analysis; K. H. and E. A. investigation; A. Y., E. A., Shohei Tanaka, Shinya Taguchi, Shunichiro Tsukamoto, H. W., K. A., and K. T. resources; K. H. and A. Y. writing—original draft; E. A., T. Y., Shohei Tanaka, Shinya Taguchi, Shunichiro Tsukamoto, H. W., K. A., and K. T. writing—review & editing; K. H. and A. Y. visualization; A. Y., H. W., K. A., and K. T. supervision; A. Y. and K. T. project administration; H. W., K. A., and K. T. funding acquisition.

**Conflict of interest**—The authors declare that they have no conflicts of interest with the contents of this article.



**Abbreviations**—The abbreviations used are: AATRAP, AT1R-associated protein; AGO, argonaute; Ang II, angiotensin II; AT1R, Ang II type 1 receptor; ATRAP, human ATRAP; Atrap, mouse Atrap; ciRPTEC, human cloned immortalized renal proximal tubule epithelial cell; DMEM, Dulbecco's modified Eagle's medium; ENaC, epithelial sodium channel; FBS, fetal bovine serum; Ho-1, heme oxygenase 1; HRP, horseradish peroxidase; IgG, immunoglobulin G; mDCT, mouse distal convoluted tubule cell; qPCR, quantitative PCR; RAS, renin-angiotensin system; RPTEC, renal proximal tubule epithelial cell; S-TuD, synthetic tough decoy; TGF $\beta$ , transforming growth factor beta.

## References

- Mills, K. T., Stefanescu, A., and He, J. (2020) The global epidemiology of hypertension. *Nat. Rev. Nephrol.* **16**, 223–237
- Chen, Y. L., and Sonkusare, S. K. (2022) Mechanosensitive angiotensin II receptor signaling in pressure-induced vasoconstriction. *J. Am. Heart Assoc.* **11**, e024740
- Zaika, O., Mamenko, M., Staruschenko, A., and Pochynyuk, O. (2013) Direct activation of ENaC by angiotensin II: recent advances and new insights. *Curr. Hypertens. Rep.* **15**, 17–24
- Coffman, T. M. (2014) The inextricable role of the kidney in hypertension. *J. Clin. Invest.* **124**, 2341–2347
- Ohsawa, M., Tamura, K., Wakui, H., Maeda, A., Dejima, T., Kanaoka, T., et al. (2014) Deletion of the angiotensin II type 1 receptor-associated protein enhances renal sodium reabsorption and exacerbates angiotensin II-mediated hypertension. *Kidney Int.* **86**, 570–581
- Horiuchi, M., Iwanami, J., and Mogi, M. (2012) Regulation of angiotensin II receptors beyond the classical pathway. *Clin. Sci. (Lond.)* **123**, 193–203
- Nehme, A., Zouein, F. A., Zayeri, Z. D., and Zibara, K. (2019) An update on the tissue renin angiotensin system and its role in physiology and pathology. *J. Cardiovasc. Dev. Dis.* **6**, 14
- Olivares-Reyes, J. A., Arellano-Plancarte, A., and Castillo-Hernandez, J. R. (2009) Angiotensin II and the development of insulin resistance: implications for diabetes. *Mol. Cell. Endocrinol.* **302**, 128–139
- Gomez, G. I., and Velarde, V. (2018) Boldine improves kidney damage in the goldblatt 2K1C model avoiding the increase in TGF-beta. *Int. J. Mol. Sci.* **19**, 1864
- Masuda, S., Tamura, K., Wakui, H., Maeda, A., Dejima, T., Hirose, T., et al. (2010) Expression of angiotensin II type 1 receptor-interacting molecule in normal human kidney and IgA nephropathy. *Am. J. Physiol. Ren. Physiol.* **299**, F720–F731
- Iwanami, J., Mogi, M., Iwai, M., and Horiuchi, M. (2009) Inhibition of the renin-angiotensin system and target organ protection. *Hypertens. Res.* **32**, 229–237
- Parving, H. H., Brenner, B. M., McMurray, J. J., de Zeeuw, D., Haffner, S. M., Solomon, S. D., et al. (2012) Cardiorenal end points in a trial of aliskiren for type 2 diabetes. *N. Engl. J. Med.* **367**, 2204–2213
- Fried, L. F., Emanuele, N., Zhang, J. H., Brophy, M., Conner, T. A., Duckworth, W., et al. (2013) Combined angiotensin inhibition for the treatment of diabetic nephropathy. *N. Engl. J. Med.* **369**, 1892–1903
- Tamura, K., Azushima, K., Kinguchi, S., Wakui, H., and Yamaji, T. (2022) ATRAP, a receptor-interacting modulator of kidney physiology, as a novel player in blood pressure and beyond. *Hypertens. Res.* **45**, 32–39
- Wakui, H., Tamura, K., Masuda, S. I., Tsurumi-Ikeya, Y., Fujita, M., Maeda, A., et al. (2013) Enhanced angiotensin receptor-associated protein in renal tubule suppresses angiotensin-dependent hypertension. *Hypertension* **61**, 1203–1210
- Ohki, K., Wakui, H., Kishio, N., Azushima, K., Uneda, K., Haku, S., et al. (2018) Angiotensin II type 1 receptor-associated protein inhibits angiotensin II-induced insulin resistance with suppression of oxidative stress in skeletal muscle tissue. *Sci. Rep.* **8**, 2846
- Azushima, K., Ohki, K., Wakui, H., Uneda, K., Haku, S., Kobayashi, R., et al. (2017) Adipocyte-specific enhancement of angiotensin II type 1 receptor-associated protein ameliorates diet-induced visceral obesity and insulin resistance. *J. Am. Heart Assoc.* **6**, e004488
- Wakui, H., Dejima, T., Tamura, K., Uneda, K., Azuma, K., Maeda, A., et al. (2013) Activation of angiotensin II type 1 receptor-associated protein exerts an inhibitory effect on vascular hypertrophy and oxidative stress in angiotensin II-mediated hypertension. *Cardiovasc. Res.* **100**, 511–519
- Wakui, H., Tamura, K., Matsuda, M., Bai, Y., Dejima, T., Shigenaga, A. I., et al. (2010) Intrarenal suppression of angiotensin II type 1 receptor binding molecule in angiotensin II-infused mice. *Am. J. Physiol. Ren. Physiol.* **299**, F991–F1003
- Matsuda, M., Tamura, K., Wakui, H., Dejima, T., Maeda, A., Ohsawa, M., et al. (2011) Involvement of Runx3 in the basal transcriptional activation of the mouse angiotensin II type 1 receptor-associated protein gene. *Physiol. Genomics* **43**, 884–894
- Subbaiah, K. C. V., Wu, J., Tang, W. H. W., and Yao, P. (2022) FAM114A1 influences cardiac pathological remodeling by regulating angiotensin II signaling. *JCI Insight* **7**, e152783
- Guo, T., Dai, Z., You, K., Battaglia-Hsu, S. F., Feng, J., Wang, F., et al. (2021) S-adenosylmethionine upregulates the angiotensin receptor-binding protein ATRAP via the methylation of HuR in NAFLD. *Cell Death Dis.* **12**, 306
- Hong, K., Zhang, Y., Yao, L., Zhang, J., Sheng, X., Song, L., et al. (2022) Pan-cancer analysis of the angiotensin II receptor-associated protein as a prognostic and immunological gene predicting immunotherapy responses in pan-cancer. *Front. Cell Dev. Biol.* **10**, 913684
- Yamaji, T., Yamashita, A., Wakui, H., Azushima, K., Uneda, K., Fujikawa, Y., et al. (2019) Angiotensin II type 1 receptor-associated protein deficiency attenuates sirtuin1 expression in an immortalised human renal proximal tubule cell line. *Sci. Rep.* **9**, 16550
- Maeda, A., Tamura, K., Wakui, H., Dejima, T., Ohsawa, M., Azushima, K., et al. (2013) Angiotensin receptor-binding protein ATRAP/Agtrap inhibits metabolic dysfunction with visceral obesity. *J. Am. Heart Assoc.* **2**, e000312
- Li, N., Wang, H. X., Han, Q. Y., Li, W. J., Zhang, Y. L., Du, J., et al. (2015) Activation of the cardiac proteasome promotes angiotensin II-induced hypertrophy by down-regulation of ATRAP. *J. Mol. Cell. Cardiol.* **79**, 303–314
- Xie, X., Shen, T. T., Bi, H. L., Su, Z. L., Liao, Z. Q., Zhang, Y., et al. (2022) Melatonin inhibits angiotensin II-induced atrial fibrillation through preventing degradation of Ang II Type I Receptor-Associated Protein (ATRAP). *Biochem. Pharmacol.* **202**, 115146
- DeCicco, D., Zhu, H., Brureau, A., Schwaber, J. S., and Vadigepalli, R. (2015) MicroRNA network changes in the brain stem underlie the development of hypertension. *Physiol. Genomics* **47**, 388–399
- O'Brien, J., Hayder, H., Zayed, Y., and Peng, C. (2018) Overview of MicroRNA biogenesis, mechanisms of actions, and circulation. *Front. Endocrinol. (Lausanne)* **9**, 402
- Friedman, R. C., Farh, K. K. H., Burge, C. B., and Bartel, D. P. (2009) Most mammalian mRNAs are conserved targets of microRNAs. *Genome Res.* **19**, 92–105
- Kim, Y. K., Kim, B., and Kim, V. N. (2016) Re-evaluation of the roles of DROSHA, export in 5, and DICER in microRNA biogenesis. *Proc. Natl. Acad. Sci. U. S. A.* **113**, E1881–E1889
- Adamcova, M., Kawano, I., and Simko, F. (2021) The impact of microRNAs in renin-angiotensin-system-induced cardiac remodelling. *Int. J. Mol. Sci.* **22**, 4762
- Menikdiwela, K. R., Ramalingam, L., Abbas, M. M., Bensmail, H., Scoggin, S., Kalupahana, N. S., et al. (2020) Role of microRNA 690 in mediating angiotensin II effects on inflammation and endoplasmic reticulum stress. *Cells* **9**, 1327
- Chen, L. J., Xu, R., Yu, H. M., Chang, Q., and Zhong, J. C. (2015) The ACE2/apelin signaling, MicroRNAs, and hypertension. *Int. J. Hypertens.* **2015**, 896861
- Sun, Y. M., Lin, K. Y., and Chen, Y. Q. (2013) Diverse functions of miR-125 family in different cell contexts. *J. Hematol. Oncol.* **6**, 6

## miR-125 inhibition represses angiotensin II signaling

36. Wang, Y., Tan, J., Wang, L., Pei, G., Cheng, H., Zhang, Q., *et al.* (2021) MiR-125 family in cardiovascular and cerebrovascular diseases. *Front. Cell Dev. Biol.* **9**, 799049
37. Nagpal, V., Rai, R., Place, A. T., Murphy, S. B., Verma, S. K., Ghosh, A. K., *et al.* (2016) MiR-125b is critical for fibroblast-to-myofibroblast transition and cardiac fibrosis. *Circulation* **133**, 291–301
38. Sakai, M., Tamura, K., Tsurumi, Y., Tanaka, Y., Koide, Y., Matsuda, M., *et al.* (2007) Expression of MAK-V/Hunk in renal distal tubules and its possible involvement in proliferative suppression. *Am. J. Physiol. Ren. Physiol.* **292**, F1526–F1536
39. Heinz, N., Schambach, A., Galla, M., Maetzig, T., Baum, C., Loew, R., *et al.* (2011) Retroviral and transposon-based tet-regulated all-in-one vectors with reduced background expression and improved dynamic range. *Hum. Gene Ther.* **22**, 166–176
40. Hafner, M., Katsantoni, M., Köster, T., Marks, J., Mukherjee, J., Staiger, D., *et al.* (2021) CLIP and complementary methods. *Nat. Rev. Methods Primers* **1**, 20
41. Kavakiotis, I., Alexiou, A., Tastsoglou, S., Vlachos, I. S., and Hatzigeorgiou, A. G. (2022) DIANA-miTED: a microRNA tissue expression database. *Nucleic Acids Res.* **50**, D1055–D1061
42. Xian, Y., Dong, L., Jia, Y., Lin, Y., Jiao, W., and Wang, Y. (2018) miR-370 promotes high glucose-induced podocyte injuries by inhibiting angiotensin II type 1 receptor-associated protein. *Cell Biol. Int.* **42**, 1545–1555
43. Haraguchi, T., Nakano, H., Tagawa, T., Ohki, T., Ueno, Y., Yoshida, T., *et al.* (2012) A potent 2'-O-methylated RNA-based microRNA inhibitor with unique secondary structures. *Nucleic Acids Res.* **40**, e58
44. Wakui, H., Tamura, K., Tanaka, Y., Matsuda, M., Bai, Y., Dejima, T., *et al.* (2010) Cardiac-specific activation of angiotensin II type 1 receptor-associated protein completely suppresses cardiac hypertrophy in chronic angiotensin II-infused mice. *Hypertension* **55**, 1157–1164
45. Ottaviani, S., Stebbing, J., Frampton, A. E., Zagorac, S., Krell, J., de Giorgio, A., *et al.* (2018) TGF-beta induces miR-100 and miR-125b but blocks let-7a through LIN28B controlling PDAC progression. *Nat. Commun.* **9**, 1845
46. Wang, S., Li, J., Wang, T., Bai, J., Zhang, Y. L., Lin, Q. Y., *et al.* (2020) Ablation of immunoproteasome beta5i subunit suppresses hypertensive retinopathy by blocking ATRAP degradation in mice. *Mol. Ther.* **28**, 279–292
47. Small, E. M., and Olson, E. N. (2011) Pervasive roles of microRNAs in cardiovascular biology. *Nature* **469**, 336–342
48. Huang, H., Zhou, J., Cui, Z., Wang, B., and Hu, Y. (2015) Angiotensin II type 1 receptor-associated protein plays a role in regulating the local renin-angiotensin system in HSC-T6 cells. *Mol. Med. Rep.* **12**, 3763–3768
49. Matsuda, M., Tamura, K., Wakui, H., Maeda, A., Ohsawa, M., Kanaoka, T., *et al.* (2013) Upstream stimulatory factors 1 and 2 mediate the transcription of angiotensin II binding and inhibitory protein. *J. Biol. Chem.* **288**, 19238–19249
50. Borem, L. M. A., Neto, J. F. R., Brandi, I. V., Lelis, D. F., and Santos, S. H. S. (2018) The role of the angiotensin II type I receptor blocker telmisartan in the treatment of non-alcoholic fatty liver disease: a brief review. *Hypertens. Res.* **41**, 394–405
51. Almutlaq, M., Alamro, A. A., Alamri, H. S., Alghamdi, A. A., and Barhoumi, T. (2021) The effect of local renin angiotensin system in the common types of cancer. *Front. Endocrinol. (Lausanne)* **12**, 736361
52. Zhang, Q., Yu, K., Cao, Y., Luo, Y., Liu, Y., and Zhao, C. (2021) miR-125b promotes the NF-kappaB-mediated inflammatory response in NAFLD via directly targeting TNFAIP3. *Life Sci.* **270**, 119071
53. Yang, X., Qiu, J., Kang, H., Wang, Y., and Qian, J. (2018) miR-125a-5p suppresses colorectal cancer progression by targeting VEGFA. *Cancer Manag. Res.* **10**, 5839–5853
54. Cao, Q., Wang, N., Ren, L., Tian, J., Yang, S., and Cheng, H. (2020) miR-125a-5p post-transcriptionally suppresses GALNT7 to inhibit proliferation and invasion in cervical cancer cells via the EGFR/PI3K/AKT pathway. *Cancer Cell Int.* **20**, 117
55. Zhang, Y., Zhang, D., Lv, J., Wang, S., and Zhang, Q. (2018) MiR-125a-5p suppresses bladder cancer progression through targeting FUT4. *Biomed. Pharmacother.* **108**, 1039–1047
56. Zheng, H., Wu, J., Shi, J., Lu, C., Wang, Y., Sun, Q., *et al.* (2017) miR-125a-5p upregulation suppresses the proliferation and induces the cell apoptosis of lung adenocarcinoma by targeting NEDD9. *Oncol. Rep.* **38**, 1790–1796
57. Hua, S., Quan, Y., Zhan, M., Liao, H., Li, Y., and Lu, L. (2019) miR-125b-5p inhibits cell proliferation, migration, and invasion in hepatocellular carcinoma via targeting TXNRD1. *Cancer Cell Int.* **19**, 203
58. Wang, Y., Wei, Y., Fan, X., Zhang, P., Wang, P., Cheng, S., *et al.* (2020) MicroRNA-125b as a tumor suppressor by targeting MMP11 in breast cancer. *Thorac. Cancer* **11**, 1613–1620
59. Friedman, P. A., and Gesek, F. A. (1995) Stimulation of calcium transport by amiloride in mouse distal convoluted tubule cells. *Kidney Int.* **48**, 1427–1434
60. Abe, E., Yamashita, A., Hirota, K., Yamaji, T., Azushima, K., Urata, S., *et al.* (2022) Angiotensin II type-1 receptor-associated protein interacts with transferrin receptor-1 and promotes its internalization. *Sci. Rep.* **12**, 17376